Journal of Medicinal Chemistry

Article

pubs.acs.org/jmc

wALADin Benzimidazoles Differentially Modulate the Function of Porphobilinogen Synthase Orthologs

Christian S. Lentz,[†] Victoria S. Halls,[‡] Jeffrey S. Hannam,[‡] Silke Strassel,[†] Sarah H. Lawrence,[§] Eileen K. Jaffe,[§] Michael Famulok,[‡] Achim Hoerauf,[†] and Kenneth M. Pfarr*[,†]

[†]Institute of Medical Microbiology, Immunology and Parasitology, University Hospital of Bonn, Sigmund-Freud Strasse 25, 53127 Bonn, Germany

[‡]Chemical Biology and Medicinal Chemistry Unit, LIMES Institute, University of Bonn, Gerhard-Domagk-Strasse 1, 53121 Bonn, Germany

[§]Fox Chase Cancer Center, Temple University Health System, 333 Cottman Avenue, Philadelphia, Pennsylvania, 19111, United States

Supporting Information

ABSTRACT: The heme biosynthesis enzyme porphobilinogen synthase (PBGS) is a potential drug target in several human pathogens. wALADin1 benzimidazoles have emerged as species-selective PBGS inhibitors against *Wolbachia* endobacteria of filarial worms. In the present study, we have systematically tested wALADins against PBGS orthologs from bacteria, protozoa, metazoa, and plants to elucidate the inhibitory spectrum. However, the effect of wALADin1 on different PBGS orthologs was not limited to inhibition: several orthologs were stimulated by wALADin1; others remained unaffected. We demonstrate that wALADins allosterically modulate the PBGS homooligomeric equilibrium with inhibition mediated by favoring low-activity oligomers, while 5-aminolevulinic acid, Mg^{2+}, or K^+ stabilized high-activity oligomers. *Pseudomonas aeruginosa* PBGS could be inhibited or stimulated by wALADin1 depending on these factors and pH. We have defined the wALADin chemotypes responsible for either inhibition or stimulation, facilitating the design of tailored PBGS modulators for potential application as antimicrobial agents, herbicides, or drugs for porphyric disorders.

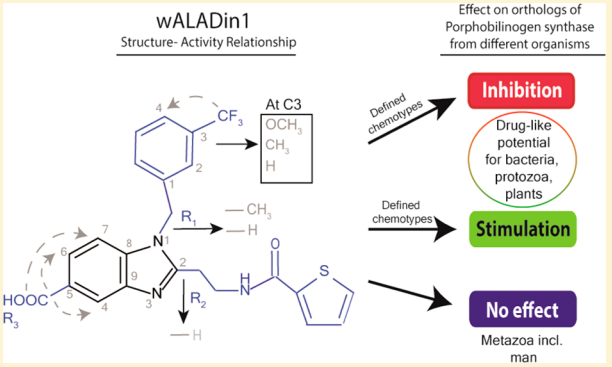

INTRODUCTION

Tetrapyrrole biosynthesis is one of the most highly conserved metabolic pathways in nature, and its final products such as heme, chlorophyll, or corrins fulfill vital functions in nearly all living organisms. A blockade of this pathway is correlated with detrimental effects not only in man, as documented by various genetic porphyric disorders and lead poisoning,[1,2] but also in many human pathogenic infections.[3−5] Eukaryotic organisms unable to synthesize heme, such as several unicellular parasites or multicellular nematodes, have molecular transporters to sequester heme from their environment or host.[6,7] For non-heme auxotrophic organisms, heme biosynthesis represents a suitable target for antiparasitic or antibacterial drugs with the precondition that the drug candidate only interferes with tetrapyrrole biosynthesis in the pathogen and not in the host.

One heme biosynthesis enzyme that shows a profound divergence in its molecular properties between different species is porphobilinogen synthase (E.C. 4.2.1.24; PBGS, also called δ-aminolevulinic acid dehydratase, ALAD).[8] PBGS synthesizes porphobilinogen by the asymmetric condensation of two molecules of 5-aminolevulinic acid (5-ALA), which is the first common step of tetrapyrrole biosynthesis.[9] Despite high sequence conservation, PBGS orthologs differ dramatically in their metal cofactor requirements[10] as well as in the stability of different quaternary structures.[8] PBGS is a homooligomeric protein with single subunits adopting an $(\alpha/\beta)_8$-barrel fold and an extended N-terminal arm that is essential for subunit−subunit interactions. Under varying environmental conditions, the subunits can adopt different conformations that support assembly into different quaternary structures with distinct catalytic activities; i.e., PBGS is a morpheein.[8,11] Mammalian, yeast, and many bacterial enzymes have a Cys-rich sequence motif that complexes catalytically essential Zn^{2+} (in the literature often referred to as $metal_B$ or Zn_B site; see also sequence alignment in Figure S1 in Supporting Information) required for binding of the second 5-ALA substrate molecule. In the plant (chloroplast) and other bacterial enzymes, this motif is replaced by a Glu-rich sequence rendering enzymatic activity of these proteins Zn^{2+}-independent. For some Zn^{2+}-

Received: November 18, 2013
Published: February 17, 2014

independent proteins (*Bradyrhizobium japanicum*,[12] *Pisum sativum*,[13] *Toxoplasma gondii*[4]) a requirement for tightly binding catalytic Mg^{2+} at the active site has been suggested, while other proteins are catalytically active in the absence of divalent metal ions (*Pseudomonas aeruginosa*,[14] *Plasmodium falciparum*,[15] *Rhodobacter capsulatus*[16]). Furthermore many orthologs are allosterically activated by Mg^{2+} binding to a conserved Glu residue (E_{245} of *P. aeruginosa* PBGS (*Pa*PBGS))[17] at an octamer-specific arm-to-barrel interface between adjacent subunits. This includes almost all Zn^{2+}-independent and many Zn^{2+}-dependent orthologs but not the human PBGS (*Hs*PBGS) or that of any metazoa or fungi.[18] Binding of Mg^{2+} to the allosteric Mg_C site stabilizes an octameric quaternary structure with high activity which is in equilibrium with dimeric or hexameric assemblies that have low activity.[19] The octameric assembly contains subunits in a conformation that allows intersubunit interactions necessary for closure of the active site lid, enabling catalysis as observed for *Pa*PBGS.[8,17,20]

We have recently reported that trisubstituted benzimidazoles of the wALADin1 family are a new class of species-discriminatory PBGS inhibitors.[21] wALADin1 is a specific inhibitor of the Mg^{2+}-responsive PBGS of the α-proteobacterium *Wolbachia*, endosymbiont in the filarial nematode parasite *Brugia malayi*, which is a drug target for treating filarial infections.[5,21,22] wALADin1 is a mixed competitive/non-competitive inhibitor that interferes with the induction of enzymatic activity by Mg^{2+}.[21] Given the specificity of this inhibitory mode of action and the insensitivity of *Hs*PBGS to this compound, wALADin1 may also be a specific inhibitor of other PBGS orthologs that are responsive to Mg^{2+} (depending on either a catalytic or allosteric Mg^{2+}). Hence, we have characterized the activity of the benzimidazole wALADin1, several wALADin1 derivatives, and the tricyclic quinoline derivative wALADin2[23] in a number of Mg^{2+}-stimulated PBGS orthologs. These included the human pathogenic or opportunistic bacteria *Escherichia coli* (*Ec*), *Vibrio cholerae* (*Vc*), *Yersinia enterocolitica* (*Ye*), *P. aeruginosa* (*Pa*), the apicomplexan parasite *Toxoplasma gondii* (*Tg*), and the chloroplast protein of *Pisum sativum* (*Ps*). As a further Mg^{2+}-independent ortholog, PBGS from the fruit fly *Drosophila melanogaster* (*Dm*) was analyzed. Depending on the PBGS class, wALADins could inhibit or stimulate activity or have no effect. Incubation of wALADin1 with the *P. aeruginosa* enzyme resulted in an inhibitory or stimulatory effect depending on the experimental conditions. Our findings suggest that modulation of PBGS activity by wALADins is likely an allosteric process that may drive the oligomeric equilibrium of these structurally flexible proteins toward a more active or less active assembly.

RESULTS

PBGS Orthologs Can Be Assigned into Three Groups Based on wALADin Cross-Species SAR. The inhibitory profile of wALADin1 (**1**), derivatives thereof (**2**−**14**), and wALADin2 (**15**) (Figure 1A−C, Table 1) against different PBGS orthologs was characterized using standardized assay conditions for each protein with constant concentrations of 1 mM $MgCl_2$ (except *Dm*PBGS) and 200 μM 5-ALA. On the basis of the outcome of modulation by wALADins, PBGS enzymes may be assigned to different groups (Figure 2): group X orthologs (containing the plant *Ps*PBGS and α-protobacterial *w*PBGS) were inhibited by wALADins (incl. wALADin2), while group Y orthologs (containing the γ-proteobacterial and

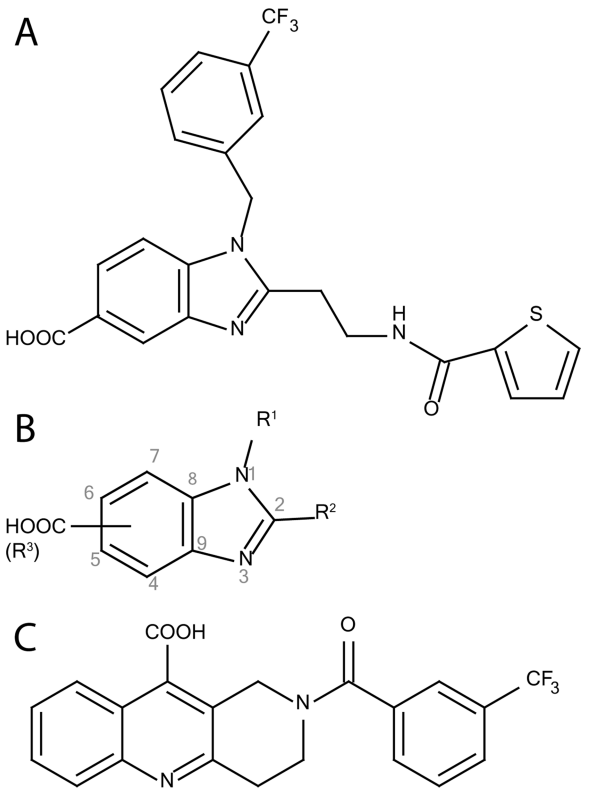

Figure 1. Chemical structures of wALADin inhibitors: (A) chemical structure of wALADin1; (B) scaffold of wALADin1 benzimidazoles described in Table 1 with atom numbering; (C) chemical structure of wALADin2.

*Tg*PBGS) were stimulated. Finally, group Z orthologs, containing Zn^{2+}-dependent PBGS orthologs from *D. melanogaster* and *H. sapiens*, were insensitive to wALADin1 (IC_{50} > 500 μM).

Activity Profile of wALADins Mediating Enzyme Inhibition of Group X PBGS. wALADin1 inhibited the plant *P. sativum* PBGS (*Ps*PBGS) with an IC_{50} of 10.6 ± 0.7 μM and was equivalent to the IC_{50} of 11.1 μM reported for the *Wolbachia* enzyme (*w*PBGS).[21] As the overall inhibitory profile of the benzimidazole derivatives against *Ps*PBGS was very similar to that of *w*PBGS, with some minor differences (summarized in Table 1 and Figure 3A), these two orthologs were classified as group X. Removal of the 2-[(2-thienylcarbonyl)amino]ethyl) substituent at R^2 (**3**) did not significantly alter inhibitory activity against either ortholog with an IC_{50} of 18.5 ± 2.4 for *Ps*PBGS and 13.0 μM for *w*PBGS. Moving the R^3-COOH from the C5 to C4 position of the benzimidazole led to a complete loss of inhibitory activity; a positional change to C6 (**4**) involved an ∼8-fold reduction of inhibitory potency (∼28-fold for *w*PBGS). Attachment of the carboxyl function to C7 (**6**) also abrogated inhibitory activity for *Ps*PBGS, which had not been observed for *w*PBGS. Alterations in the 3-CF_3-benzyl R^1 substituent led to a quantitatively similar impairment of inhibitory activity in both orthologs. However, compound **13** with a methyl group as the R^1 substituent had weak inhibitory activity against *Ps*PBGS (IC_{50} = 257 ± 46 μM) but not against *w*PBGS. wALADin2 (**15**) was ∼10-fold less potent at inhibiting *Ps*PBGS (IC_{50} = 88.2 ± 8.0 μM) compared with *w*PBGS (IC_{50} = 8.1 μM[23]).

Elucidation of the mode of action of wALADin1 against *Ps*PBGS determined a mixed competitive/noncompetitive

dx.doi.org/10.1021/jm401785n | J. Med. Chem. 2014, 57, 2498−2510

Table 1. Activity Profile of wALADin1 Benzimidazoles and wALADin2 on Group X PBGS (*P. sativum, Wolbachia*) vs Group Z PBGS (*D. melanogaster, H. sapiens*)

				group X PBGS IC_{50} [μM]		group Z PBGS IC_{50} [μM]	
compd	R_1 residue	R_2 residue	position of R_3 residue	*Ps*PBGS (R^2)	*w*PBGS[b]	*Dm*PBGS (R^2)	*Hs*PBGS[b]
1 (wALADin1)	3-CF_3-benzyl	2-[(2-thienylcarbonyl)amino]ethyl	C5	10.6 ± 0.7 (0.9852)	11.1	1111 ± 77 (0.9594)	~739
2	H	2-[(2-thienylcarbonyl)amino]ethyl	C5	114 ± 13 (0.9297)	*a*	448 ± 45 (0.9628)	*a*
3	3-CF_3-benzyl	H	C5	18.5 ± 2.4 (0.9512)	13.0	340 ± 31 (0.9685)	197
4	3-CF_3-benzyl	2-[(2-thienylcarbonyl)amino]ethyl	C6	89.0 ± 7.3 (0.9623)	317	257 ± 21 (0.9666)	*a*
5	3-CF_3-benzyl	2-[(2-thienylcarbonyl)amino]ethyl	C4	*a*	*a*	*a*	*a*
6	3-CF_3-benzyl	2-[(2-thienylcarbonyl)amino]ethyl	C7	*a*	164	*a*	*a*
7	4-CF_3-benzyl	2-[(2-thienylcarbonyl)amino]ethyl	C5	44.3 ± 5.0 (0.9555)	38.6	1008 ± 373 (0.7024)	~637
8	4-CF_3-benzyl	H	C5	43.1 ± 1.9 (0.9885)	87.7	620 ± 87 (0.9021)	173
9	2-CF_3-benzyl	H	C5	64.3 ± 5.3 (0.9639)	293	*a*	145
10	benzyl	H	C5	182 ± 13 (0.9715)	197	1033 ± 400 (0.9170)	213
11	3-CH_3-benzyl	H	C5	95.9 ± 6.0 (0.9806)	134	371 ± 45 (0.9515)	222
12	3-OCH_3-benzyl	H	C5	155 ± 16 (0.9473)	205	370 ± 93 (0.8125)	156
13	CH_3	H	C5	257 ± 46 (0.8557)	*a*	*a*	*a*
14	H	H	C5	*a*	*a*	*a*	511
15 (wALADin2)		tricyclic quinoline derivative		88.2 ± 8.0 (0.9631)	8.1[c]	*a*	*a, c*

[a]No inhibitory activity; $IC_{50} \gg 500$ μM for *Ps*PBGS, *w*PBGS, *Hs*PBGS; $IC_{50} \gg 1$ mM for *Dm*PBGS, *w*PBGS, and *Hs*PBGS. For *Dm*PBGS IC $\gg 1$ mM. Highest concentration tested: 533 μM for PsPBGS; 1.2 mM for *Dm*PBGS. [b]Values for compounds **1**–**14** are from ref 21. [c]Value for compound **15** is from ref 23.

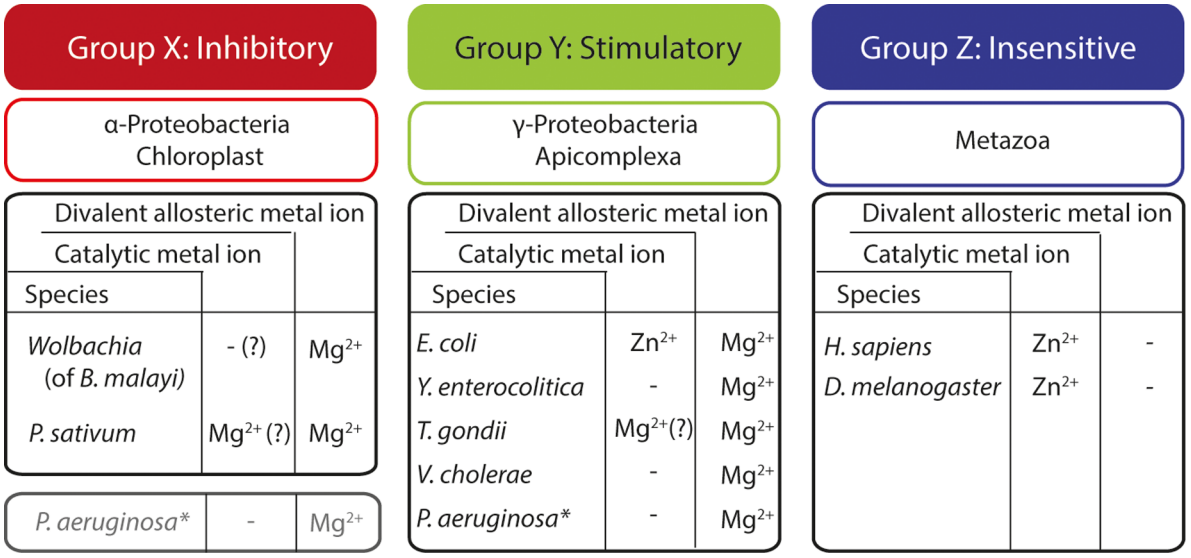

Figure 2. Three classes of PBGS ortholog groups according to the structure–activity relationship of wALADin1. Group X PBGS orthologs from *Wolbachia* and *P. sativum* are inhibited by wALADin1 benzimidazoles. Group Y PBGS orthologs from *E. coli, V. cholera, Y. enterocolitica, P. aeruginosa,* and *T. gondii* are stimulated by wALADin1 benzimidazoles. The metazoan group Z PBGS orthologs from *D. melanogaster* and *H. sapiens* are insensitive to wALADin1 benzimidazoles. SAR data for *Hs*PBGS and *w*PBGS were reported in ref 21. The asterisk (*) indicates that *Pa*PBGS was originally assigned to group Y, but it must also, in part, be counted among group X because it was inhibited by wALADin1 under certain experimental conditions (see Figure 4, Figure S4), and it is therefore also listed in gray below the inhibited group X orthologs.

mechanism and partial competition with the activation induced by Mg^{2+} (parts A–C of Figure S2) as seen with the *Wolbachia* protein.[21] At a saturating concentration of 10 mM 5-ALA, wALADin1 also induced a decrease of the maximum activity of *w*PBGS in a Mg^{2+}-response curve (part D of Figure S2). Thus, the effect of wALADin1 on *w*PBGS involves both a reduction in affinity for Mg^{2+} and a reduction in enzymatic velocity when Mg^{2+} is bound. At 100 μM wALADin1 the affinity for Mg^{2+} was 18.6-fold lower for *w*PBGS but only 2.2-fold for *Ps*PBGS.

Activity Profile of wALADins Mediating Enzyme Activation of Group Y PBGS. The other PBGS orthologs tested were from the γ-proteobacteria *E.coli, P. aeruginosa, V. cholerae, Y. enterocolitica,* and the apicomplexan parasite *T. gondii*. These orthologs were stimulated rather than inhibited by wALADin1 and several other wALADin derivatives and therefore were assigned to group Y. The compounds that exerted a stimulating effect on these enzymes were wALADin1, the R^3 positional isomers **4** (R^3-COOH at C6, for *Ye* and *Tg* only), **5** (R^3-COOH at C4), **6** (R^3-COOH at C7, for *Ye* and *Tg* only), and the R^1 positional isomer **7** (R^1-4-CF_3-benzyl) (Table 2, Figure 3B). Enzymatic activity was stimulated to a maximum of 15–42% over control reactions treated with 6.7% DMSO,

dx.doi.org/10.1021/jm401785n | J. Med. Chem. 2014, 57, 2498–2510

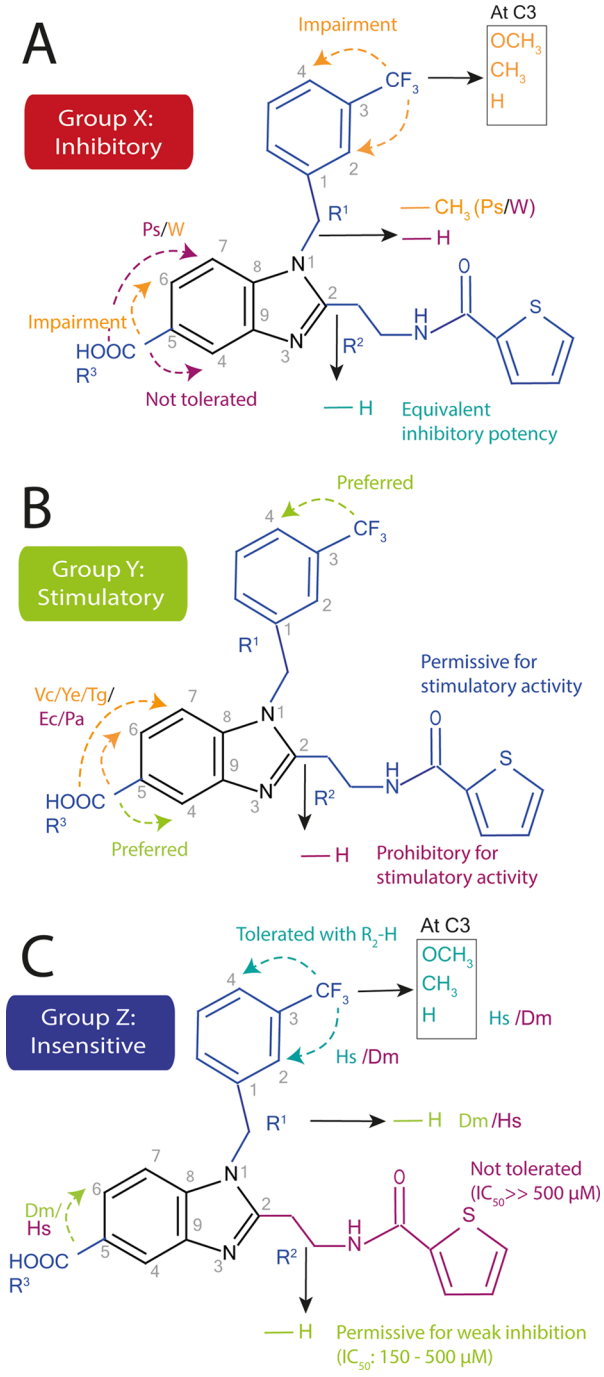

Figure 3. Summary of SAR on PBGS groups X, Y, and Z: (A) SAR data for inhibition of group X (*Wolbachia* and *P. sativum*); (B) stimulation of group Y orthologs (*E.coli*, *P. aeruginosa*, *V. cholerae*, *Y. enterocolitica*, and *T. gondii*); (C) insensitive group Z containing *Hs*PBGS and *Dm*PBGS. The benzimidazole core is shown in black, and substituents of the parent molecule wALADin1 are in blue. Positional changes of residues are indicated by dashed arrows, and chemical changes in substituents are indicated with black solid arrows. The consequences of chemical alterations with respect to biological activity are highlighted in color: green (similar or improved activity), orange (reduced activity), or purple (abrogated activity). When the effects of a structural modification varied for different members of a group, the species abbreviations are given in the corresponding colored font: *W* = *Wolbachia*, *Ps* = *P. sativum*, *Ec* = *E. coli*, *Vc* = *V. cholerae*, *Ye* = *Y. enterocolitica*, *Pa* = *P. aeruginosa*, *Tg* = *T. gondii*, *Hs* = *H. sapiens*, *Dm* = *D. melanogaster*. Data from *w*PBGS and *Hs*PBGS were reported in ref 21.

Table 2. Stimulatory Activity of wALADin1 Benzimidazoles on Various PBGS Orthologs

	Escherichia coli			*Vibrio cholerae*			*Yersinia enterocolitica*			*Pseudomonas aeruginosa*			*Toxoplasma gondii*		
compd	EC_{50} [μM]	max stim [%][b]	R^2	EC_{50} [μM]	max stim [%][b]	R^2	EC_{50} [μM]	max stim [%][b]	R^2	EC_{50} [μM]	max stim [%][b]	R^2	EC_{50} [μM]	max stim [%][b]	R^2
1	60 ± 21	120.5	0.8488	182 ± 154	160	0.6501	66 ± 12	151.7	0.8853	~69[c]	122.8[c]	0.6404[c]	95 ± 42	128.0	0.9224
4	*a*	100		*d*	115.3[d]	*d*	*d*	131.2[d]		*a*	100		*d*	115.2[d]	*d*
5	19 ± 9	116	0.8227	38 ± 26	117	0.6598	23 ± 2	123.2	0.9230	15 ± 21	135.6	0.8227	21 ± 3	130.0	0.9448
6	*a*	100		*d*	113.3[d]	*d*	*d*	118.2[d]		*a*	100		*d*	112.9[d]	*d*
7	39 ± 16	128	0.7482	53 ± 29	117	0.6598	52 ± 13	142.2	0.8387	68 ± 21	139.5	0.6921	37 ± 13	117.6	0.8363
other	*a*	100		*a*	100		*a*	100		*a*	100		*a*	100	

[a]No stimulatory or inhibitory activity. Highest concentration tested: 533 μM. *Vc*PBGS was weakly inhibited by compounds **12** (IC_{50} ≈ 1400 ± 624 μM; R^2 = 0.6392) and **13** (IC_{50} ≈ 843 ± 236 μM; R^2 = 0.8639). [b]Activity data were normalized, and control reactions performed in the presence of 6.7% DMSO instead of compound were set to 100% activity. [c]Data from the highest concentration tested (533 μM) were excluded from nonlinear regression because biological activity started to decline, and thus, the nonlinear fit of the data was ambiguous. [d]Stimulation was only achieved at the highest concentration tested (533 μM). The corresponding value is reported as the maximum stimulation value, although higher concentrations of compound may lead to a further increase in enzymatic activity. Because of their low potency, no EC_{50} values could be determined for these compounds.

dx.doi.org/10.1021/jm401785n | J. Med. Chem. 2014, 57, 2498−2510

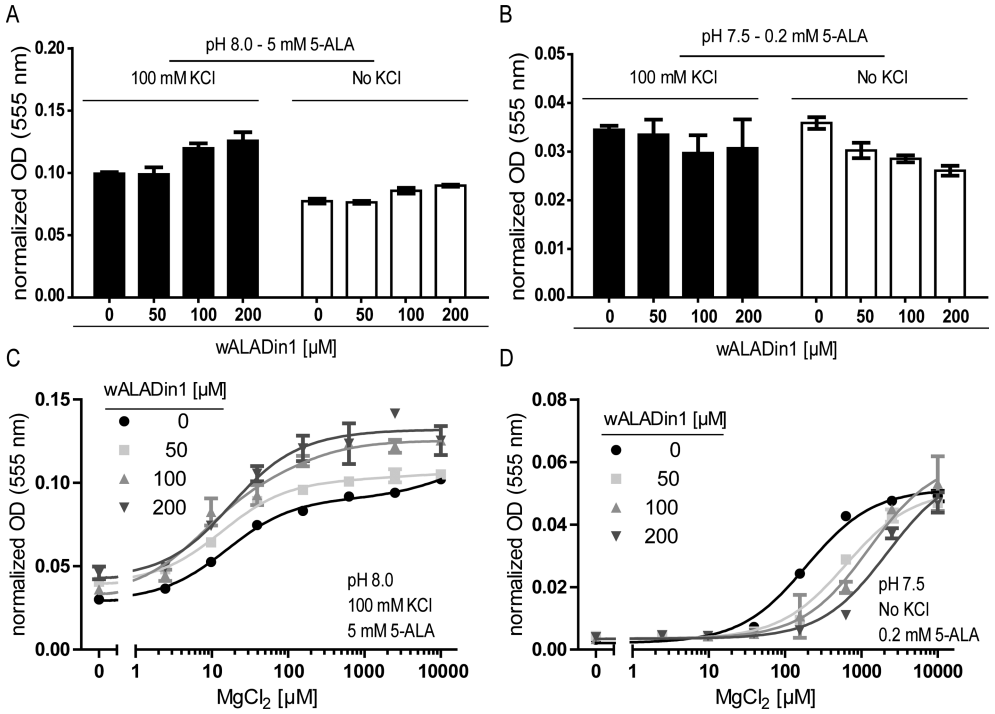

Figure 4. Stimulatory and inhibitory effects of wALADin1 on *Pa*PBGS. In a buffer scan experiment testing various pH and 5-ALA and KCl concentrations (all tested conditions are shown in Figure S4), experimental conditions were defined under which wALADin1 (A) stimulated *Pa*PBGS activity (pH 8.0, 5 mM 5-ALA, 100 mM KCl) or (B) inhibited *Pa*PBGS activity (pH 7.5, 0.2 mM 5-ALA, no KCl). (C) Under the given stimulatory conditions, increasing [Mg^{2+}] resulted in an increased V_{MAX} in the presence of wALADin1. The effect on the Mg^{2+} $K_{0.5}$ was not consistent (compare 100 to 200 μM). (D) Under inhibitory conditions, the Mg^{2+}-response curve was shifted to the right by increasing [wALADin1]. Curves were fit by nonlinear regression assuming a sigmoidal (four-parameter) progression.

corresponding to EC_{50} values between 20 and 300 μM according to nonlinear regression (NLR) analysis. NLR gave in part weak fits (R^2 = 0.64−0.92) probably due to the low extent of stimulation in combination with high EC_{50} values. In contrast to the preferred "inhibitory chemotype" described above for *Ps*/*w*PBGS, the exchange of the R^2-2[(2-thienylcarbonyl)amino]ethyl) moiety to -H was not tolerated. None of the compounds lacking this moiety stimulated enzymatic activity. Although derivative **5** (R^3-COOH at C4) was completely inactive against *Ps*/*w*PBGS, it was, together with compound **7** (R^1-4-CF_3-benzyl), the most potent stimulator of enzymatic activity.

Group Z PBGSs Are Insensitive to wALADins. The activity of the Zn^{2+}-dependent fruit fly *Dm*PBGS ortholog was insensitive to wALADin1 (IC_{50} > 1000 μM, Table 1) and is therefore assigned to group Z, along with the likewise wALADin1-insensitive *Hs*PBGS (as reported in ref 21). *Dm*PBGS and *Hs*PBGS have a very similar SAR profile (Table 1, Figure 3C) with the majority of wALADin1 derivatives featuring the R^2- 2[(2-thienylcarbonyl)amino]ethyl) moiety being ineffective. The only exceptions are **2** (with an R^1-H instead of 3-CF_3-benzyl; IC_{50}(*Dm*PBGS) = 448 ± 45 μM) and **4** (a positional isomer with R^3-COOH at C_6; IC_{50}(*Dm*PBGS) = 257 ± 21 μM) that inhibit *Dm*PBGS but not *Hs*PBGS. As described previously for *Hs*PBGS,[21] also for *Dm*PBGS, replacement of the R^2-2[(2-thienylcarbonyl)amino]-ethyl) by a hydrogen atom in **3** led to a ~3-fold gain in inhibitory activity (IC_{50} = 340 ± 31 μM) compared to the parent molecule. Within the series of R^2-H compounds with alterations in the R^1-position permissive for inhibition of *Hs*PBGS, only R^1-3-CH_3-benzyl (**11**, IC_{50} = 371 ± 45 μM), R^1-3-O-CH_3 (**12**, IC_{50} = 370 ± 93 μM), and weakly R^1-4-CF_3-benzyl (**8**, IC_{50} = 620 ± 93 μM) but not R^1-2-CF_3-benzyl (**9**) or R^1-benzyl (**10**) were tolerated by *Dm*PBGS.

Inferring Group Membership for Other PBGS Orthologs from Protein Sequence Information. Multiple sequence alignment of the full length proteins did not reveal molecular motifs that could clearly define group membership (Figure S1). While all orthologs assigned to either group X or group Y feature an allosteric Mg_C, neither of the metazoan group Z orthologs responds to Mg^{2+}; rather both require Zn^{2+}. Among group Y PBGS orthologs, the *E. coli* enzyme requires catalytic Zn_B (Figure S1 [24]) while the other proteins do not require catalytic divalent cations (Figure S1 [4,10,14,25]). The pattern of oligomeric states sampled by these orthologs is also inconsistent, e.g., dimer and octamer for *P. aeruginosa*[26] and *T. gondii*,[4] while the *E. coli*[25] and *Y. enterocolitica* proteins (E.K. Jaffe, unpublished observation) can sample the hexamer. The *V. cholerae* PBGS samples another higher order multimeric assembly in addition to the octamer (E. K. Jaffe, unpublished observation).

***Rickettsia* and *Chlamydia* PBGS Are Likely Susceptible to Inhibition by wALADins.** *Wolbachia* are obligate intracellular bacteria related to *Rickettsia* spp.[27] and *Chlamydia* spp.,[28] several of which are disease agents in humans. Since the respective PBGS orthologs have not been recombinantly produced, we were unable to include them in our analysis of wALADin activity. Therefore, we performed an in silico analysis.

A phylogenetic analysis (maximum likelihood method) of the protein sequences of tested PBGS orthologs is shown in Figure S3. Inclusion of PBGS protein sequences from pathogenic,

dx.doi.org/10.1021/jm401785n | J. Med. Chem. 2014, 57, 2498−2510

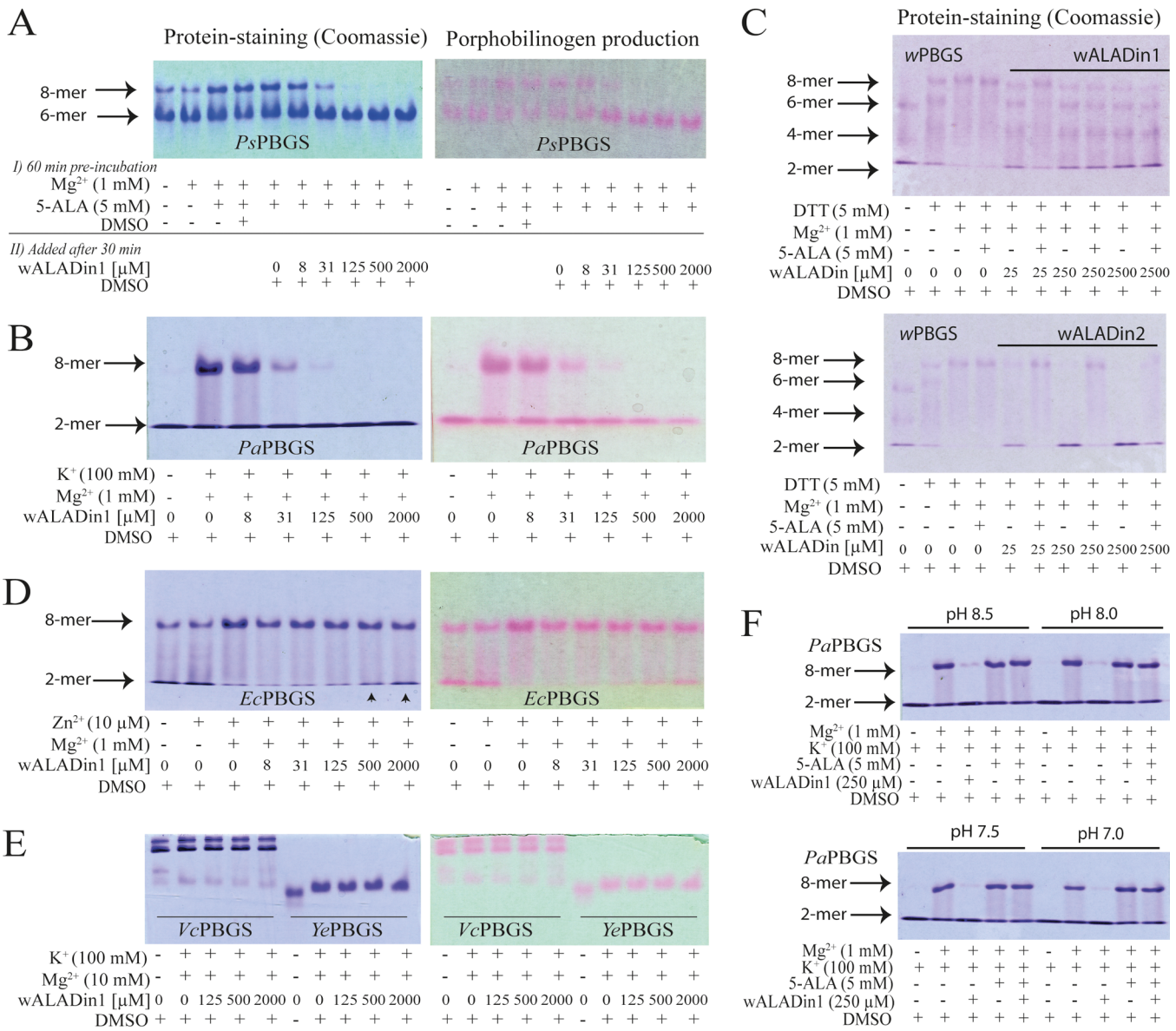

Figure 5. Nondenaturing PAGE analysis of PBGS orthologs. (A) 2 μg of *Ps*PBGS, (B, F) 3 μg of *Pa*PBGS, (C) 2 μg of *w*PBGS, (D) 3 μg of *Ec*PBGS, or (E) 2 μg *Vc*PBGS and 2 μg *Ye*PBGS were incubated for 60 min (*Ps*PBGS) or 20 min (all other proteins) at 37 °C in the respective optimal buffer containing the indicated concentrations of K^+, Mg^{2+}, Zn^{2+}, 5-ALA, and wALADin1 before samples were loaded onto a 7.5% nondenaturing PAGE gel. After gel electrophoreis, an in-gel activity assay was conducted (A, B, D, E). Protein bands were stained with Coomassie Blue (left panel), and porphobilinogen production was detected with Ehrlich's reagent (right panel). (A) Incubation of *Ps*PBGS with 5 mM 5-ALA for 60 min shifted the oligomeric equilibrium from the hexamer toward the octamer. Addition of wALADin1 after 30 min followed by further preincubation for 30 min reverted this transition and locked the protein in the hexameric assembly. (B) In the presence of 1 mM Mg^{2+} and 100 mM K^+ a large amount of *Pa*PBGS assembled into the octameric state, whereas incubation with wALADin1 induced enzymatically inactive dimers. (C) *w*PBGS was incubated with different concentrations of DTT, Mg^{2+}, or 5-ALA in the absence/presence of wALADin1 (upper gel) or wALADin2 (lower gel). wALADin1 shifted the equilibrium away from octamer and induced all dimeric, tetrameric, and hexameric assemblies, while wALADin2 induced the dimer only. (D) High concentrations of wALADin1 (2 mM) weakly induced the low molecular weight (putatively dimeric) population of *Ec*PBGS (arrowheads). (E). wALADin1 had no influence on the oligomeric equilibrium of *Vc*PBGS or *Ye*PBGS. (F) *Pa*PBGS was incubated for 30 min at 37 °C in different pH buffers (100 mM Tris-HCl, 100 mM KCl, pH 7.0−8.5) in the presence/absence of 1 mM Mg^{2+}, 5 mM 5-ALA, and wALADin1. The octamer-inducing effect of 5 mM 5-ALA dominated the dimer-inducing effect of 250 μM wALADin1.

obligate intracellular α-proteobacteria *Rickettsia rickettsii* and *R. prowazekii* (Figure S3) confirms their close relationship to the *Wolbachia* protein, suggesting that these orthologs are susceptible to inhibition by wALADin1. Two members of obligate intracellular bacteria of the Chlamydiae family (*Chlamydia pneumonia* and *C. trachomatis*) are located in a more isolated branch most closely related to the chloroplast *P. sativum* protein and the plastid-derived *T. gondii* ortholog (Figure S3). PBGS from both *Rickettsia* and *Chlamydia* are predicted to be Zn^{2+}-independent and to possess an allosteric Mg^{2+}-binding site consistent with group X orthologs.

***P. aeruginosa* PBGS Can Be Inhibited or Stimulated by wALADin1 Depending on the Experimental Conditions.** As a model for stimulated group Y orthologs, the protein from *P. aerguinosa*, one of the best characterized PBGS proteins, was analyzed in more detail. A buffer scan experiment was carried

dx.doi.org/10.1021/jm401785n | J. Med. Chem. 2014, 57, 2498−2510

out to monitor the influence of pH and concentrations of 5-ALA and KCl on the effect of wALADin1 on *Pa*PBGS (Figure S4). This experiment revealed that the stimulatory effect of wALADin1 that prevailed under standard conditions (Figure 4A) was inhibitory in the absence of K^+, low pH, and low 5-ALA concentrations, (Figure 4B, Figure S4). A similar buffer scan experiment for the other group Y orthologs from *E. coli*, *V. cholerae*, and *Y. enterocolitica* did not reveal conditions that resulted in inhibitory activity of the wALADin1 (parts A−C of Figure S5).

We aimed to determine whether the wALADin1 activity profile for *Pa*PBGS under inhibitory conditions was comparable to that described above for stimulatory conditions (Table 2) or whether it was more similar to that of group X PBGS (Table 1) by determining the IC_{50} concentrations for selected derivatives: wALADin1 (IC_{50} = 79 ± 3 μM); **3** (94 ± 4 μM); **5** (no inhibitory activity, highest concentration tested, =533 μM), wALADin2 (475 ± 31 μM). Although the compounds had a generally weaker activity on *Pa*PBGS (under inhibitory conditions) compared to *Ps*PBGS and *w*PBGS, the activity profile of wALADins revealed key characteristics of group X orthologs: dispensability of the R^2-2[(2-thienylcarbonyl)-amino]ethyl) (compare wALADin1 to **3**), inactivity of the R^3-COOH positional isomer **5**, and the effectiveness of wALADin2.

***P. aeruginosa* PBGS: Mg^{2+}, K^+, and 5-ALA Reduce the Inhibitory Effect of wALADin1, and K^+ Is Required for wALADin1-Elicited Stimulation.** We proceeded to characterize the influence of the different buffer components on *Pa*PBGS activation and inhibition under "standard stimulatory" (100 mM Tris-HCl, pH 8.0, 1 mM $MgCl_2$, 5 mM 5-ALA, 100 mM KCl) and "standard inhibitory" conditions (100 mM Tris-HCl, pH 7.5, 1 mM $MgCl_2$, 0.2 mM 5-ALA, no KCl) in more detail.

The inhibitory effect was similar to that described for similar *Ps*PBGS and *w*PBGS. Under "standard inhibitory" conditions wALADin1 functionally competed with Mg^{2+} (Figure 4 D), but in contrast to group X PBGS (parts C and D of Figure S2), maximum activity of *Pa*PBGS was restored at high Mg^{2+} (10 mM). As *Pa*PBGS does not require catalytic metal ions but is allosterically activated by Mg^{2+},[14] this indicates that wALADin1 reduces the affinity for the allosteric Mg^{2+} or stabilizes a form of the protein with a lower affinity for the allosteric Mg^{2+} (e.g., pro-octamer dimer). Under "standard stimulatory" conditions the affinity of *Pa*PBGS for Mg^{2+} was not consistently altered, but V_{MAX} was increased (Figure 4C).

Monovalent K^+ had been reported to have an activating effect on *Pa*PBGS function[14] and was included at high concentration in the buffer used for the EC_{50} determinations described above. K^+-dilution series under "standard stimulatory" and "standard inhibitory" conditions revealed that this monovalent cation is required to achieve a stimulatory effect of wALADin1 (part A of Figure S6) while antagonizing the inhibitory effect (part B of Figure S6). Binding studies using thermal shift assays conducted in the presence and absence of K^+ showed that this ion had no influence on the binding of wALADin1 to *Pa*PBGS (parts C and D of Figure S6). We conclude that the conformational changes of *Pa*PBGS or the selection of certain assembly states elicited by K^+-binding[20] might alter the functional outcome of wALADin1-binding.

Classic Michaelis−Menten kinetics demonstrated that under "standard stimulatory" conditions, K_M was not affected, while V_{MAX} was increased (part A of Figure S7). Under "standard inhibitory" conditions increasing [wALADin1] led to a consistent increase in K_M, indicating competition with 5-ALA; however, V_{MAX} was only reduced at low inhibitor concentrations (part B of Figure S7). This pattern was also observed in the initial buffer scan experiments (Figure S4). This non-canonical behavior might indicate binding of wALADin1 with a different affinity and functional outcome to (a) different binding sites or (b) the same binding site in different subpopulations of protein (e.g., different oligomeric states or different protomers of one oligomer).

wALADin1 Mediates Inhibition by Stabilizing Inactive Low Molecular Weight Assemblies in the Oligomeric Equilibrium of PBGS Orthologs. PBGS is a morpheein and therefore can form a variety of different oligomeric states including dimers, hexamers, or octamers specific for each ortholog.[8] To elucidate whether the inhibitory or stimulatory activity of wALADin1 on PBGS proteins is associated with stabilization of certain oligomer populations, proteins were preincubated with a dilution series of wALADin1 and the oligomers were separated by nondenaturing PAGE (Figure 5). Activity of the protein oligomers in the gel was measured by incubating the gel in an activity stain buffer that included 5-ALA, followed by in-gel staining for porphobilinogen production with Ehrlich's reagent. wALADin1 shifted the *Ps*PBGS oligomeric equilibrium away from the high-activity octameric state to the low-activity hexameric assembly (Figure 5A) and thus likely conferred inhibition. Porphobilinogen production by *Ps*PBGS was not reduced in the in-gel activity assay (Figure 5A, right panel), probably because the excess of 5-ALA in the buffer had displaced previously bound wALADin1 from the protein (according to the mixed inhibition model) which then diffused away from the protein reducing the local concentration. 5-ALA is known to induce a transition from hexameric or dimeric protein to the active octamer for various PBGS orthologs.[8] Therefore, the enzymatic activity of protein in the hexameric band most likely resulted from a 5-ALA-induced transition from hexameric to octameric protein in the gel, as we have previously shown using a 2D native gel technique.[25,29] wALADin2 also led to a stabilization of *Ps*PBGS hexamers, although with weaker affinity than wALADin1 (data not shown).

A very similar effect was observed for *Pa*PBGS. Preincubation with Mg^{2+} and K^+ alone led to a shift from the putative dimeric to the octameric assembly and induced a population with high enzymatic activity (Figure 5B). Figure S8 shows a structural representation of the *Pa*PBGS octamer highlighting the binding interfaces of both allosteric Mg^{2+} and K^+. In our native PAGE assays, the octamer-inducing effect of Mg^{2+} and K^+ and the corresponding enzymatic activity were abrogated by wALADin1 in a concentration-dependent manner (Figure 5B). As the predominantly resulting dimeric protein is expected to be enzymatically inactive, any porphobilinogen production at this location, again, likely arose from in-gel transition to octamers induced by 5-ALA. At wALADin1 concentrations of ≥500 μM all of the protein was present as a dimer (Figure 5B, left panel) and had a decreased ability to produce porphobilinogen as demonstrated by the in-gel assay (Figure 5B, right panel), indicating that the inhibitor successfully prevented the 5-ALA induced assembly of dimers into octamers during the activity assay. These results for *Pa*PBGS and *Ps*PBGS demonstrated that wALADin1 allosterically modulates PBGS structure and, for these orthologs, locks the protein in its inactive assembly state as the molecular basis for inhibition.

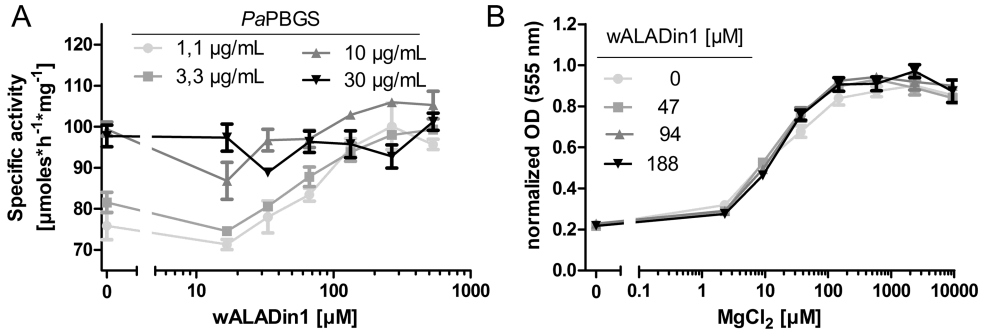

Figure 6. Protein-concentration-dependent specific activity of *Pa*PBGS and wALADin1 stimulation: (A) wALADin1 dose−response curves recorded under "standard stimulatory" assay conditions (100 mM Tris-HCl, pH 8.0, 10 mM $MgCl_2$, 100 mM KCl, 5 mM 5-ALA); (B) Mg^{2+}-response curve for 10 µg/mL *Pa*PBGS under the same conditions described in part A. The stimulatory effect of wALADin1 disappeared at this protein concentration.

However, this mechanism is in disagreement with our previous observation that wALADin1 did not interfere with the oligomeric equilibrium of *w*PBGS but bound to and inhibited octameric protein.[21] In those experiments preincubation had been performed in 1× protein loading buffer containing glycerol and bromophenol blue that may have obscured an effect of wALADin1 on the *w*PBGS oligomeric equilibrium. We therefore reanalyzed the effect of wALADin1 on this endobacterial ortholog using the current protocol where protein loading buffer was added after preincubation. *w*PBGS was found to exist in an equilibrium of at least four different assemblies including potential dimeric, tetrameric, hexameric, and octameric states (Figure 5C, upper panel). The addition of DTT, Mg^{2+}, and 5-ALA preferentially induced the octamer, while wALADin1 induced all the inactive lower molecular weight assemblies. While 5 mM 5-ALA was still able to reverse the effect of 25 µM wALADin1, higher concentrations of wALADin1 dominated the oligomeric equilibrium and prevented the octamer-inducing effect of 5-ALA. In contrast to the benzimidazole wALADin1, the tricyclic quinoline derivative wALADin2 strongly induced the dimer but stabilized neither tetramers nor hexamers (Figure 5C, lower panel) and was easily overcome by excess 5-ALA. Thus, the inhibitory mechanism for both wALADin1 and wALADin2 is also stabilization of inactive assembly states of *w*PBGS.

Stimulatory Effect of wALADin1 on Group Y PBGS Is Protein Concentration-Dependent. In analogy, the stimulatory effect by wALADin1 observed for some PBGS orthologs might be elicited by a stabilization of the active octameric state and a concurrent increase in enzymatically active protein. However, native PAGE experiments did not reveal evidence for a wALADin1-elicited stabilization of octamers for either of the group Y PBGS orthologs that might explain the stimulatory activity of the compound (Figure 5B,D−F). For *Ec*PBGS the highest wALADin1 concentrations reduced the Mg^{2+}-stimulated conversion of dimer to octamer (Figure 5D, left panel), whereas neither the oligomeric equilibrium of *Vc*PBGS nor that of *Ye*PBGS was markedly altered by preincubation with wALADin1 (Figure 5E). As described above, we observed stabilization of *Pa*PBGS dimers (Figure 5B) under conditions that, in the enzymatic assay, led to stimulation, not inhibition.

Importantly, while present in the enzymatic assay, 5-ALA was omitted during the preincubation period for the native PAGE experiments on *Pa*PBGS shown in Figure 5B. We therefore determined the effect of wALADin1 on *Pa*PBGS at different pH values and in the presence and absence of 5 mM 5-ALA (Figure 5F). While the octamer-stabilizing effect of Mg^{2+} and 5-ALA and a pH dependency (high pH favors octamers, low pH favors hexamers) were readily observed, no octamer-stabilizing effect of wALADin1 was discerned under any condition. But while wALADin1 was able to stabilize the *Pa*PBGS dimer in the absence of 5-ALA, 5 mM 5-ALA completely abrogated this effect (Figure 5 F), demonstrating that the status of the oligomeric equilibrium (as influenced by 5-ALA and the pH) dominates the outcome of modulation by wALADin1. As the percentage of enzymatic activation achieved by wALADin1 was generally very low (∼20%), it is uncertain whether such minor differences would be properly reflected by a nonquantitative method such as native PAGE.

Alternatively, it was possible that the stimulation of catalytic activity by wALADin1 resulted from a mechanism increasing the catalytic rate of pre-existing octamers rather than increasing the percentage of octamers in the equilibrium. In that instance the stimulatory effect of wALAD1 should be additive to conditions that promote octamer formation. PBGS is known to exhibit a protein-concentration-dependent specific activity with higher protein concentrations promoting octamer formation.[20,30] wALADin1 dose−response curves in the presence of saturating and nonsaturating *Pa*PBGS concentrations revealed that the specific activity of *Pa*PBGS ("standard stimulatory" conditions with 10 mM $MgCl_2$) increased with protein concentration until a maximum activity of ∼(100 µmol of porphobilinogen)·h^{-1}·(mg of protein)$^{-1}$ was reached at ∼10 µg/mL protein (Figure 6A). These specific activity values were identical to those values achieved by stimulation of wALADin1 at lower protein concentrations. At saturating protein concentrations with maximum specific activity, wALADin1 had no additional stimulatory properties (Figure 6A), which was confirmed over the entire range in a Mg^{2+}-dilution series (Figure 6B). Similar findings were seen for *Vc*PBGS, *Ye*PBGS, and *Ec*PBGS (data not shown). These data suggest that wALADin1 and an increase in protein concentration have functionally redundant effects in promoting an active octameric assembly, although the final experimental proof of octamer stabilization by wALADin1 still has to be provided (compare Figure 5D−F).

■ DISCUSSION AND CONCLUSIONS

Products of the tetrapyrrole biosynthesis pathway fulfill essential biological functions in nearly all organisms, and a blockade of this pathway may provoke serious malfunction or

dx.doi.org/10.1021/jm401785n | J. Med. Chem. 2014, 57, 2498−2510

death. Because of the generally high degree of conservation of the involved enzymes among different species, this pathway has been difficult to exploit for the design of antibiotics, antifungal, antiparasitic, herbicidal, or pest control agents intended to specifically interfere with tetrapyrrole biosynthesis of the target organisms without affecting that of humans.

In the current study we have tested the recently discovered class of wALADins, species-specific inhibitors of an endobacterial (*Wolbachia* of *Brugia malayi*) PBGS,[21] against a variety of PBGS orthologs in in vitro enzymatic inhibition tests to determine the potential effector spectrum on different organisms. Using the different orthologs, we found two contrasting biological effects elicited by wALADins, i.e., inhibition and stimulation. The susceptibility to these two effects allows one to assign the different PBGS orthologs into three categories: Group X PBGS orthologs are inhibited by wALADin1; group Y PBGS orthologs are stimulated; Group Z members are neither potently inhibited nor stimulated. It must be noted that inhibitory and stimulatory susceptibilities are not mutually exclusive for a single protein, as demonstrated for the *P. aeruginosa* enzyme, for which the position of the oligomeric equilibrium determines whether wALADins inhibit or stimulate.

Our results provide important insight into the molecular mechanism by which wALADins act, as exemplified mostly for wALADin1. We would first like to address the inhibitory mechanism. Different PBGS orthologs are known to sample different oligomeric states, with the common feature that equilibria of low and high activity assemblies exist.[8] The high activity states are usually octamers, while dimers and hexamers have been described as the inactive assemblies because they lack subunit interactions required to stabilize a closed conformation of the active site lid. The interconversion between hexamers and octamers involves disassembly to two conformationally distinct forms of dimers (pro-octamer and pro-hexamer dimers) with an intrinsic propensity to assemble into octamers or hexamers, respectively. For all inhibited group X PBGS orthologs we have demonstrated that wALADin1 disturbs the oligomeric equilibrium of these proteins, thus stabilizing the low activity hexamers (*Ps*PBGS), dimers (*Pa*PBGS), or a variety of low molecular weight assemblies (*w*PBGS). Our previous finding that wALADin1 had no effect on the oligomeric equilibrium of *w*PBGS[21] may be ascribed to the presence of 20% glycerol in the preincubation buffer that may have led to artificial stabilization of the octamer. Thus, wALADin1 can be classified as a "morphlock" inhibitor that locks a morpheein in its inactive assembly state and thus confers inhibition.[31] Such molecules have previously been detected by targeted in silico screening[26,31,32] or screening in an in vitro gel shift assay.[33] In contrast, wALADin1 was originally identified by an unbiased enzymatic assay screening for inhibitors.[21] This serendipitous finding of a morphlock inhibitor indicates the potential that oligomeric state regulators of morpheeins have for inhibitor design.

Not only the SAR profiles of *Ps*PBGS and *w*PBGS are highly analogous, but the proteins also share a mixed competitive/noncompetitive mode of inhibition by wALADin1, involving a functional competition with Mg^{2+} (this study and ref 21). This mode of action may be explained using the morpheein model involving regulation of the oligmeric equilibrium.[8] Both Mg^{2+} and 5-ALA induce the active octameric form and are thus in competition with wALADin1 that stabilizes the inactive assemblies. It is interesting to note that wALADin1 induced a wide range of *w*PBGS oligomeric assemblies, whereas wALADin2 only induced the dimer. The differential stabilization pattern of certain subsets of oligomers may explain the different results obtained for wALADin1 and wALADin2 when determining the mode of inhibition by enzyme kinetics.[21,23]

In contrast to previously described morphlocks, which inhibit by stabilizing inactive PBGS assemblies,[26,31−33] most stimulatory influence on the protein is mediated via an induction of the highly enzymatically active octameric assembly, as is the case for allosteric Mg^{2+} and K^+ binding (see structural representation in Figure S8), active site binding of 5-ALA[8,30] and high protein concentrations (a phenomenon known as protein concentration-dependent specific activity[12,13,20,30]). In order to achieve a stimulatory effect, wALADin1 must bind to and stabilize the octamers (or pro-octamer dimers) of group Y PBGS orthologs, and it is plausible that the stimulatory effect of wALADin1 is also mediated by stabilization of octamers. Although we were not able to directly demonstrate that stimulation of group Y PBGS is mediated via an induction of the octameric assembly in native PAGE assays, enzymatic assays revealed that wALADin1-mediated stimulation was abolished or strongly diminished at high protein concentrations. This indicates that wALADin1 does not increase the catalytic rate of a single octamer but rather modifies the oligomeric equilibrium in a way that promotes the assembly of, and/or stabilizes, enzymatically active oligomers. This effect apparently becomes redundant with high PBGS concentration when the octamer is strongly induced. Yet it remains to be determined which equilibrium constants of the oligomerization pathway are affected by wALADin1 binding and how this effect differs from and integrates with the octamer-inducing influence of Mg^{2+} or 5-ALA.

The *P. aeruginosa* protein showed the peculiarity that it was both inhibited and stimulated by wALADin1 as a function of pH, 5-ALA, and KCl. Apparently, the modulator is able to bind both to the dimeric and octameric assembly, which is likely to occur with different affinities and different on- and off-rates. In the absence of 5-ALA, wALADin1 drove the oligomeric equilibrium toward the inactive dimeric state, whereas high concentrations of 5-ALA abrogated this effect, shifting the equilibrium toward the octamer. Thus, the overall effect of wALADin1-mediated modulation depends on the initial status of the oligomeric equilibrium. In the absence of strong octamer-inducing stimuli (such as 5-ALA) the dimer-stabilizing effect prevails. In contrast, when the dimer concentration falls below a certain threshold (e.g., at high 5-ALA, which is supported by high pH, Mg^{2+}, and K^+), wALADin1 may bind predominantly to the octamer (or pro-octamer dimer or intermediates), temporarily stalling the protein in this assembly and facilitating the formation of active octamers which will become visible as a net stimulation effect. This model may explain the noncanonical progression of the substrate-response curve (Figures S4 and S7) where, under otherwise identical buffer conditions, the elevated 5-ALA concentration turned an inhibitory effect by wALADin1 into stimulation.

In order to fully support the suggested modes of action a cocrystal structure of a PBGS enzyme with a bound wALADin modulator will be required. To date, attempts to crystallize the *Wolbachia* or pea protein have not been successful. In contrast, for the *P. aeruginosa* protein[17,34] and various group Y PBGS, like that from *E. coli*[24] and *T. gondii*,[35] crystal structures are available. Hence, solution of a crystal structure of the *P. aeruginosa* PBGS with wALADin1 bound may be the most

facile approach to initially determine the wALADin binding site. Such cocrystallization studies are currently in progress.

All members of a PBGS group are inhibited/stimulated by a defined chemotype of wALADin1 benzimidazoles that share an SAR profile, which markedly differs from that of the other groups. This is illustrated best by focusing on the R^2-2[(2-thienylcarbonyl)amino]ethyl) substituent and its replacement by a hydrogen atom. For group X orthologs this alteration had a minor effect, but it abrogated activity on group Y, while it weakly increased activity on metazoan group Z orthologs. A specific activity profile was also observed for the tricyclic quinoline derivative wALADin2, which only inhibited members of the group X PBGS. Interestingly, the activity profile of wALADins for *Pa*PBGS under stimulatory conditions was like that of other group Y PBGS; however, under inhibitory conditions it was similar to that of group X PBGS. We therefore conclude that the difference between the stimulatory and inhibitory outcome is not merely functional. Thus, under the two conditions, structurally distinct wALADin-binding sites are exposed that have a different binding preference for a chemotype, i.e., for group X or group Y PBGS. These distinct binding environments are likely related to certain states of the oligomeric equilibrium.

It is remarkable that the only two orthologs (*H. sapiens* and *D. melanogaster*) that did not feature an allosteric Mg^{2+}-binding site were not affected by wALADin1, whereas all Mg^{2+}-responsive orthologs were inhibited or stimulated. Beyond that, neither the requirement of PBGS enzymes for catalytic metal ions nor the predicted oligomeric architectures of the orthologs revealed an unambiguous pattern with respect to wALADin1-responsiveness and did not allow for a clear prediction of this property. Thus, based on the activity spectrum presented in this study, phylogenetics (Figure S3) may be the most promising approach for predicting the activity of wALADins to PBGS of different species. The PBGS of *T. gondii* is targeted to the apicoplast,[4] a nonphotosynthetic plastid found in apicomplexan parasites that has been acquired through secondary endosymbiosis of a red alga and is likely of cyanobacterial origin.[36,37] It is therefore interesting that *Tg*PBGS responds to wALADin1 treatment similar to the γ-proteobacterial orthologs and not to the chloroplast-derived pea enzyme. A unique feature of *Tg*PBGS is the presence of a C-terminal extension that stabilizes the octameric assembly and does not sample the hexamer.[35] As wALADin1 mediates inhibition of plastid *Ps*PBGS by stabilizing the hexamer, the absence of this assembly from the *Tg*PBGS oligomeric equilibrium may be an explanation for the lack of inhibitory activity of wALADins against this apicomplexan PBGS.

The species-specific inhibition of wALADins on group X PBGS might be exploited for drug development, provided that in vivo tests confirm the efficacy of these heme biosynthesis inhibitors. Group X comprises the *Wolbachia*, *P. sativum*, and in part the *P. aeruginosa* ortholog. In addition to the already demonstrated activity of wALADin1 on filarial worms (that contain and are dependent upon *Wolbachia* endosymbionts)[21] our phylogenetic analysis indicates that PBGS from other intracellular α-proteobacterial pathogens closely related to *Wolbachia*, such as *Rickettsia* spp.[27] are likely susceptible to inhibition by wALADin1. *Chlamydia*[28] PBGS orthologs are most closely related to the chloroplast protein of pea and the apicoplast protein of *T. gondii*, followed by the *Wolbachia* protein. In the absence of the C-terminal extension such as that of the *T. gondii* ortholog that mediates octamer stabilization and may render the protein insusceptible to wALADin1-induced dimer-stabilization, it is likely that the *Chlamydia* orthologs behave more like the *P. sativum* protein which is susceptible to inhibition by wALADin1 via hexamer stabilization. Confirmation of the antibiotic potential of wALADins against *Rickettsia* and *Chlamydia* (causing, for example, typhus, Rocky Mountain spotted fever, and sexually transmitted chlamydia) would require purification of the respective recombinant proteins and in vitro drug tests in the enzymatic assay and bacterial culture and is outside the scope of this study. PBGS of photosynthetic eukaryotes such as *P. sativum* are targeted to the chloroplast and are phylogenetically related as they are believed to have arisen from a common ancestor.[10,38] The inhibitory activity of wALADins on the pea protein therefore indicates that wALADins might be potential herbicides. For the *P. aeruginosa* protein the major factor rendering the enzyme insusceptible to inhibition by wALADin1 (and instead promoting stimulation) is high substrate concentrations. Depending on the bacterial physiology, it is possible that an inhibitory effect of wALADin1 may occur in vivo, which might affect bacterial viability or virulence. In the setting of prolonged PBGS inhibition, it is possible that 5-ALA may eventually accumulate above the threshold to overcome the inhibition (turning the outcome to stimulation). Yet because of pro-oxidative effects, elevated 5-ALA levels might have a toxic effect on the bacterium similar to what we have observed previously for filarial nematode in culture[21] and as reported in the context of various human disorders.[39]

The stimulatory activity of wALADin1 and a number of its derivatives on the PBGS enzymes from several γ-proteobacteria (*E. coli*, *V. cholerae*, *Y. enterocolitica*) and the apicomplexan parasite *T. gondii* adds another layer of complexity (and specificity) to wALADins. Because of the stimulatory effects on PBGS of these organisms, a potential therapeutic use of wALADin-like compounds might appear challenging, unless overproduction of porphyrins and precursors has a (photo)-toxic effect on these organisms as is observed with several forms of porphyria.[1] If future research is able to translate the concept of PBGS stimulation also to the human enzyme, this might open new avenues for the therapy of diseases characterized by reduced PBGS activity, like lead poisoning, through (partial) rescue of the catalytic rate of porphobilinogen formation via stimulation by wALADin-like compounds.

The comprehensive analysis of the diverse biological effects of wALADin modulators on different PBGS orthologs, elucidation of the corresponding chemical profiles of the small molecules, and mechanistic insights presented in this work will provide the groundwork for the development of tailored inhibitors or activators of heme biosynthesis with potential therapeutic applications.

EXPERIMENTAL SECTION

Proteins. The *Vibrio cholerae* (*Vc*PBGS, UniProtKB C3LPU7), *Yersinia enterocolitica* (*Ye*PBGS, F4MUJ9), *Escherichia coli* (*Ec*PBGS, P0ACB2), *Drosophila melanogaster* (*Dm*PBGS, Q9VTV9), and *Pisum sativum* (*Ps*PBGS, P30124) proteins were recombinantly expressed in their native form without purification tags. The general method for protein purification was as follows (details follow below). Bacterial cells were disrupted, and the PBGS protein was precipitated using ammonium sulfate. The redissolved ammonium sulfate pellet was applied to a phenyl Sepharose-CL4B column that had been equilibrated in ammonium sulfate/potassium phosphate. Following a reverse ionic strength gradient, PBGS protein eluted at 2 mM KPi, pH 7.0. The pool of active protein was then applied to and further purified

on a Q-sepharose column using a gradient from low to high ionic strength. In some cases the Q-Sepharose column separated different quaternary structure isoforms (e.g., octamer and hexamer), and these isolated pools, though quite pure by SDS−PAGE, may have undergone further purification on a Sephacryl S-300 column or a Superdex 200 column. Column buffers generally contained the divalent metal ions required/used by the various PBGS. The full details of the purification of *Ps*PBGS, *Dm*PBGS, and *Ec*PBGS have been published.[13,18,40]

*Vc*PBGS, expressed in *E. coli* from a pET3 vector construct, was purified using a 20−40% ammonium sulfate cut; active protein was applied to and purified on a phenyl Sepharose column (4 °C; elution gradient from 30 mM potassium phosphate, pH 7.5, 15% ammonium sulfate to 2 mM potassium phosphate, pH 7.5) and a Q-Sepharose column (room temperature; elution gradient from 30 mM Tris-HCl, pH 7.0, 1 mM $MgCl_2$ to 30 mM Tris-HCl, pH 7.0, 10 mM $MgCl_2$, 0.4 M KCl). All buffers used for the phenyl Sepharose and Q-Sepharose columns also contained 10 mM 2-mercaptoethanol and 0.1 mM phenylmethylsulfonyl fluoride. The final step, a Sephacryl S-300 column, was run in 0.1 M Tris-HCl, pH 7, 10 mM $MgCl_2$, 10 mM 2-mercaptoethanol.

*Ye*PBGS, was expressed in *E. coli* from a pET3 vector construct and purified using a 15−30% ammonium sulfate cut; active protein was applied to and purified on a phenyl Sepharose column (4 °C; elution gradient from 30 mM potassium phosphate, pH 7.5, 5% ammonium sulfate to 2 mM potassium phosphate, pH 7.5) and a Q-Sepharose column (room temperature; elution gradient from 10 mM Tris-HCl, pH 7.0 to 1 M Tris-HCl, pH 7.0). As above, all buffers used for the phenyl Sepharose and Q-Sepharose columns contained 10 mM 2-mercaptoethanol and 0.1 mM phenylmethylsulfonyl fluoride.

Wolbachia of *Brugia malayi* PBGS (*w*PBGS, Q5GSR3) was expressed with a C-terminal His-tag as described.[5,21] For recombinant expression of the *P. aeruginosa* ortholog (*Pa*PBGS, Q59643) the *hemB* gene of *P. aeruginosa* strain PA01 (kindly provided by Dr. B. Henrichfreise, Bonn, Germany) was amplified by PCR with a primer set including NdeI and XhoI restriction sites in the forward and reverse primers, respectively: *Pa*PBGS-NdeI-Fw_primer, 5′-GTCATATGAGCTTCACTCCCGCC-3′; *Pa*PBGS-XhoI-Rv_primer, 5′-GTCTCGAGACGCCCCCGTCTTAATTGTTCT-3′. All primers were purchased from Biolegio (Nijmegen, The Netherlands). The forward primer was modified from Frankenberg et al.[41] PCR reactions were performed using 500 nM primers, 200 μM dNTPs, 0.02 U Phusion Taq (New England Biolabs, Ipswich, MA, USA) in 1× Phusion buffer HF (New England Biolabs) using the following amplification protocol: initial denaturation at 98 °C for 5 min followed by 35 amplification cycles (98 °C for 10 s, 72 °C for 80 s). After gel purification, the amplified DNA fragment (∼1 kb) was cloned into the pET-21b vector (Merck Chemicals, Darmstadt, Germany) encoding a His_6-tag downstream of the XhoI restriction site. The expression plasmid was transformed into BL21 *E. coli* (Life Technologies, Darmstadt, Germany). Bacterial cultures were grown at 37 °C, 150 rpm until an OD_{600} of 0.5−0.6 when protein expression was induced with 100 μM isopropyl β-D-1-thiogalactopyranoside (IPTG; Fermentas, St. Leon-Rot, Germany) for 24 h at room temperature, 150 rpm. His-tagged *w*PBGS and *Pa*PBGS were purified with Ni-NTA-Agarose (Qiagen, Hilden, Germany) following the manufacturer's protocol. *w*PBGS and *Pa*PBGS were stored in 100 mM Tris-HCl, pH 8.0, 300 mM NaCl, 25 mM imidazole, 10% glycerol.

The *T. gondii hemB* gene was cloned and expressed as described by Shanmugam et al.[4] with minor modifications using the following primers: *Tg*PBGS-NdeI-FW primer, 5′-TATACATATGACGCCACGGGGGCCCCTCGAC-3′; *Tg*PBGS-BamHI-RV primer, 5′-GATGGATCCTTAGTAGCAGGGTTCTGTAAACTTCTGC-3′. In brief, the amplified sequence was cloned into the pET-21b vector, which was then transformed into BL21 *E. coli*. Bacterial cultures were grown as above until OD_{600} = 0.6 when protein expression was induced with 100 μM IPTG overnight at 23 °C, 180 rpm. Protein was purified following the general protocol by Shanmugam et al.[4] involving sonication, iterative freeze−thaw cycles, an ammonium sulfate cut, and sequential purification on a phenyl-Sepharose CL-4B and a Q Sepharose high performance column. Protein was finally eluted with gradient of 10 mM to 1 M Tris-HCl, pH 7.0, 1 mM $MgCl_2$. Fractions containing active protein were pooled, concentrated to 0.22 mg/mL, and stored at −80 °C.

Enzymatic Assays. PBGS activity assays were performed as described previously.[21,23] In brief, reactions were incubated in activity buffer (see below) with 5-ALA (Sigma Aldrich, Munich, Germany) at 36 °C for 10−60 min. The reaction was stopped by addition of 200 μL of modified Ehrlich's reagent (1 g of 4-dimethylaminobenzaldehyde (Sigma, Munich, Germany) dissolved in 42 mL of acetic acid, 12 mL of perchloric acid, and 7.3 mL of 12% trichloroacetic acid), incubated at room temperature for 10 min, and the OD_{555} was read. IC_{50} determinations of wALADin1 and its derivatives for the different PBGS orthologs were performed under buffer conditions optimal for each protein, all with 0.2 mM 5-ALA. These concentrations had previously been used in IC_{50} determinations for *w*PBGS, for which inhibitory activity was dependent on Mg^{2+} and 5-ALA concentration.[21] Protein concentrations and reaction times were adjusted to ensure a maximum substrate turnover of 30%. This required subsaturating PBGS concentrations at which protein-concentration-dependent differences in the specific activity of the protein may prevail because of the equilibrium of different quaternary assemblies of PBGS. Thus, the standard reaction conditions for the different orthologs were as follows. All protein concentrations are listed as subunit concentrations and specific activities under the given conditions are indicated in brackets:

(1) *Ec*PBGS: 200 nM protein in 100 mM Bis-Tris propane (BTP)-HCl, pH 8.1, 1 mM $MgCl_2$, 10 μM $ZnCl_2$, 5 mM DTT for 10 min [∼(85.1 μmol of porphobilinogen)/(mg of protein·h)]
(2) *Ps*PBGS: 300 nM protein in 100 mM BTP-HCl, pH 8.5, 1 mM $MgCl_2$, 5 mM DTT for 15 min [∼(11.4 μmol of porphobilinogen)/(mg of protein·h)]
(3) *Vc*PBGS: 125 nM protein in 100 mM BTP-HCl, pH 8.0, 1 mM $MgCl_2$, 5 mM DTT, 100 mM KCl for 10 min [∼(32.7 μmol of porphobilinogen)/(mg of protein·h)]
(4) *Ye*PBGS: 150 nM protein in 100 mM BTP-HCl, pH 8.0, 1 mM $MgCl_2$, 5 mM DTT, 100 mM KCl for 10 min [∼(25.7 μmol of porphobilinogen)/(mg of protein·h)]
(5) *Pa*PBGS: 150 nM protein in 100 mM Tris-HCl, pH 8.0, 1 mM $MgCl_2$, 100 mM KCl for 10 min [∼(19.3 μmol of porphobilinogen)/(mg of protein·h)]
(6) *Tg*PBGS: 250 nM protein in 100 mM Tris-HCl, pH 8.0, 1 mM $MgCl_2$, 5 mM DTT for 20 min [∼(8.9 μmol of porphobilinogen)/(mg of protein·h)]
(7) *Dm*PBGS: 400 nM protein in 100 mM BTP-HCl pH 8.0, 0.5 μM $ZnCl_2$, 100 μM DTT for 60 min. [∼1.0 μmol porphobilinogen/(mg protein * hour)]

Compounds. Benzimidazole compounds **1**−**14** were synthesized as described previously.[21] Compound **15**[23] was purchased from Peakdale Ltd. (Chapel-en-le-Frith, U.K.). The purity of the compounds was determined on an Agilent 1100 series HPLC (Agilent, Germany) using a C18 Eclipse XDB-C18 column (4.6 mm × 150 mm, Agilent) by applying a gradient of doubly distilled H_2O up to 100% acetonitrile in 25 min (flow rate, 1 mL/min). All compounds had a purity of ≥95%.

Nondenaturing PAGE. PBGS proteins were preincubated for 10 min at 37 °C in their respective enzymatic assay buffer (see above) containing different concentrations of Mg^{2+}, K^+, 5-ALA, Zn^{2+}, and wALADin1. Samples were then put on ice, and 2× protein loading buffer was added (0.2 M Tris-HCl, pH 8.8, 40% glycerol, 0.005% bromophenol blue). An amount of 2−3 μg of protein was loaded onto a 7.5% nondenaturing PAGE gel (1× gel buffer, 7 mM Tris-HCl, 7 mM sodium acetate, pH 6.5) and run at 20−25 V, 25 mA, 4 °C for 15−20 h (running buffer, 25 mM Tris-HCl, pH 8.8, 80 mM glycine). For monitoring of in-gel enzymatic activity, the gels were soaked in activity stain buffer (see below), incubated for 10−15 min at 36 °C and porphobilinogen was stained with modified Ehrlich's reagent (see above). Gels were scanned on a flatbed scanner, quickly rinsed in H_2O and stained with Coomassie Blue for 20 min, destained with 30%

methanol for 2 h to overnight, and scanned again. Activity stain buffer composition was as follows: *Pa*PBGS, 100 mM Tris-HCl (pH 8.0), 100 mM KCl, 1 mM $MgCl_2$, 500 μM 5-ALA; *Ps*PBGS, 100 mM BTP-HCl (pH 8.5), 1 mM $MgCl_2$, 100 μM DTT, 500 μM 5-ALA; *Ec*PBGS, 100 mM BTP (pH 8.1), 1 mM $MgCl_2$, 100 μM $ZnCl_2$, 100 μM DTT, 500 μM 5-ALA; *Vc*PBG/*Ye*PBGS, 100 mM BTP-HCl (pH 8.0), 100 mM KCl, 10 mM $MgCl_2$, 100 μM DTT, 500 μM 5-ALA.

Software and Data Analyses. Data were analyzed with Prism 5.02 for Windows (GraphPad Software, San Diego, CA, USA). Half maximal inhibitory concentration values (IC_{50}) were determined by fitting logarithmical data to the "log(inhibitor) vs normalized response − variable slope" algorithm $[Y = 100/(1 + 10^{((\log IC_{50} - X)h)})]$ with h as the Hill coefficient. Half maximal effective concentration values for stimulatory effects ("EC_{50}" stimulation induced by wALADins on several PBGS orthologs) were fit with the "log(agonist) vs response − variable slope" algorithm $[Y = \text{Bottom} + (\text{Top} - \text{Bottom})/(1 + 10^{((\log EC_{50} - X)h)})]$. The binding constant for Mg^{2+} ($K_{0.5}$) was approximated from activity data using the same equation. Data from substrate concentration series were fit individually by nonlinear regression assuming conventional Michaelis−Menten kinetics $[Y = V_{MAX}X/(K_M + X)]$, K_M being the Michaelis−Menten constant and V_{MAX} being the maximum enzymatic velocity. Eadie−Hofstee transformation followed by linear regression was performed for a linearized representation of these data. If not stated otherwise, graphs show the mean ± SD from triplicate measurements. Figure S8 was prepared from the Protein Data Bank file 1GZG (http://www.rcsb.org/pdb/explore.do?structureId=1GZG) using the PyMOL Molecular Graphics System, version 1.3, from Schrödinger, LLC.

■ ASSOCIATED CONTENT

Supporting Information

Multiple sequence alignment of orthologous PBGS protein sequences (Figure S1); inhibition of *Ps*PBGS and *w*PBGS by wALADin1 (Figure S2); phylogeny of PBGS (Figure S3); effect of KCl, pH, and [5-ALA] on wALADin1 activity against *Pseudomonas aeruginosa* PBGS (Figure S4); pH screen of stimulated *Vc*-, *Ye*-, and *Ec*PBGS orthologs (Figure S5); effect of K^+ on the interaction of PaPBGS and wALADin1 (Figure S6); Michaelis−Menten kinetics of PaPBGS (Figure S7); structural representation of Mg^{2+}- and K^+-binding sites in the PaPBGS octamer (Figure S8). This material is available free of charge via the Internet at http://pubs.acs.org.

■ AUTHOR INFORMATION

Corresponding Author

*Phone: +49 228 287 11207. Fax: +49 228 287 11167. E-mail: pfarr@microbiology-bonn.de.

Author Contributions

The manuscript was written through contributions of all authors. All authors have given approval to the final version of the manuscript.

Notes

The authors declare no competing financial interest.

■ ACKNOWLEDGMENTS

This work was supported through a grant from the Liverpool School of Tropical Medicine to A.H. and K.M.P as part of the A-WOL Consortium funded by the Bill and Melinda Gates Foundation, the Deutsche Forschungsgemeinschaft (Grant SFB 704) to A.H. and M.F, and by the U.S. National Institutes of Health Grants ES003654 and AI077577 (E.K.J.). We thank Linda Stith for technical assistance with protein expression and purification.

■ ABBREVIATIONS USED

5-ALA, 5-aminolevulinic acid; ALAD, δ-aminolevulinic acid dehydratase; *Dm*, *Drosophila melanogaster*; *Ec*, *Escherichia coli*; *Hs*, *Homo sapiens*; *Pa*, *Pseudomonas aeruginosa*; PBGS, porphobilinogen synthase; *Ps*, *Pisum sativum*; SAR, structure−activity relationship; SD, standard deviation; *Tg*, *Toxoplasma gondii*; *Vc*, *Vibrio cholerae*; *w*, *Wolbachia* of *Brugia malayi*; *Ye*, *Yersinia enterocolitica*

■ REFERENCES

(1) Balwani, M.; Desnick, R. J. The porphyrias: advances in diagnosis and treatment. *Blood* **2012**, *120*, 4496−4504.

(2) Warren, M. J.; Cooper, J. B.; Wood, S. P.; Shoolingin-Jordan, P. M. Lead poisoning, haem synthesis and 5-aminolaevulinic acid dehydratase. *Trends Biochem. Sci.* **1998**, *23*, 217−221.

(3) Koreny, L.; Obornik, M.; Lukes, J. Make it, take it, or leave it: heme metabolism of parasites. *PLoS Pathog.* **2013**, *9*, e1003088.

(4) Shanmugam, D.; Wu, B.; Ramirez, U.; Jaffe, E. K.; Roos, D. S. Plastid-associated porphobilinogen synthase from *Toxoplasma gondii*: kinetic and structural properties validate therapeutic potential. *J. Biol. Chem.* **2010**, *285*, 22122−22131.

(5) Wu, B.; Novelli, J.; Foster, J.; Vaisvila, R.; Conway, L.; Ingram, J.; Ganatra, M.; Rao, A. U.; Hamza, I.; Slatko, B. The heme biosynthetic pathway of the obligate *Wolbachia* endosymbiont of *Brugia malayi* as a potential anti-filarial drug target. *PLoS Negl. Trop. Dis.* **2009**, *3*, e475.

(6) Chen, C.; Samuel, T. K.; Krause, M.; Dailey, H. A.; Hamza, I. Heme utilization in the *Caenorhabditis elegans* hypodermal cells is facilitated by heme-responsive gene-2. *J. Biol. Chem.* **2012**, *287*, 9601−9612.

(7) Tripodi, K. E.; Menendez Bravo, S. M.; Cricco, J. A. Role of heme and heme-proteins in trypanosomatid essential metabolic pathways. *Enzyme Res.* **2011**, *2011*, 873230.

(8) Jaffe, E. K.; Lawrence, S. H. Allostery and the dynamic oligomerization of porphobilinogen synthase. *Arch. Biochem. Biophys.* **2012**, *519*, 144−153.

(9) Jaffe, E. K. The porphobilinogen synthase catalyzed reaction mechanism. *Bioorg. Chem.* **2004**, *32*, 316−325.

(10) Jaffe, E. K. An unusual phylogenetic variation in the metal ion binding sites of porphobilinogen synthase. *Chem. Biol.* **2003**, *10*, 25−34.

(11) Jaffe, E. K. Morpheeins—a new structural paradigm for allosteric regulation. *Trends Biochem. Sci.* **2005**, *30*, 490−497.

(12) Petrovich, R. M.; Litwin, S.; Jaffe, E. K. *Bradyrhizobium japonicum* porphobilinogen synthase uses two Mg(II) and monovalent cations. *J. Biol. Chem.* **1996**, *271*, 8692−8699.

(13) Kervinen, J.; Dunbrack, R. L., Jr.; Litwin, S.; Martins, J.; Scarrow, R. C.; Volin, M.; Yeung, A. T.; Yoon, E.; Jaffe, E. K. Porphobilinogen synthase from pea: expression from an artificial gene, kinetic characterization, and novel implications for subunit interactions. *Biochemistry* **2000**, *39*, 9018−9029.

(14) Frankenberg, N.; Jahn, D.; Jaffe, E. K. *Pseudomonas aeruginosa* contains a novel type V porphobilinogen synthase with no required catalytic metal ions. *Biochemistry* **1999**, *38*, 13976−13982.

(15) Dhanasekaran, S.; Chandra, N. R.; Chandrasekhar Sagar, B. K.; Rangarajan, P. N.; Padmanaban, G. Delta-aminolevulinic acid dehydratase from *Plasmodium falciparum*: indigenous versus imported. *J. Biol. Chem.* **2004**, *279*, 6934−6942.

(16) Bollivar, D. W.; Clauson, C.; Lighthall, R.; Forbes, S.; Kokona, B.; Fairman, R.; Kundrat, L.; Jaffe, E. K. *Rhodobacter capsulatus* porphobilinogen synthase, a high activity metal ion independent hexamer. *BMC Biochem.* **2004**, *5*, 17.

(17) Frankenberg, N.; Erskine, P. T.; Cooper, J. B.; Shoolingin-Jordan, P. M.; Jahn, D.; Heinz, D. W. High resolution crystal structure of a Mg^{2+}-dependent porphobilinogen synthase. *J. Mol. Biol.* **1999**, *289*, 591−602.

(18) Kundrat, L.; Martins, J.; Stith, L.; Dunbrack, R. L., Jr.; Jaffe, E. K. A structural basis for half-of-the-sites metal binding revealed in

Drosophila melanogaster porphobilinogen synthase. *J. Biol. Chem.* **2003**, *278*, 31325−31330.
(19) Breinig, S.; Kervinen, J.; Stith, L.; Wasson, A. S.; Fairman, R.; Wlodawer, A.; Zdanov, A.; Jaffe, E. K. Control of tetrapyrrole biosynthesis by alternate quaternary forms of porphobilinogen synthase. *Nat. Struct. Biol.* **2003**, *10*, 757−763.
(20) Jaffe, E. K.; Lawrence, S. H. The Dance of Porphobilinogen Synthase in the Control of Tetrapyrrole Biosynthesis. In *Handbook of Porphyrin Science*; Ferreira, C. G., Kadish, K. M., Smith, K. M., Guilard, R., Eds.; World Scientific Publishing Co.: Hackensack, NJ, 2013; Vol. *26*, pp 80−129.
(21) Lentz, C. S.; Halls, V.; Hannam, J. S.; Niebel, B.; Strubing, U.; Mayer, G.; Hoerauf, A.; Famulok, M.; Pfarr, K. M. A selective inhibitor of heme biosynthesis in endosymbiotic bacteria elicits antifilarial activity in vitro. *Chem. Biol.* **2013**, *20*, 177−187.
(22) Taylor, M. J.; Hoerauf, A.; Bockarie, M. Lymphatic filariasis and onchocerciasis. *Lancet* **2010**, *376*, 1175−1185.
(23) Lentz, C. S.; Stumpfe, D.; Bajorath, J.; Famulok, M.; Hoerauf, A.; Pfarr, K. M. New chemotypes for wALADin1-like inhibitors of delta-aminolevulinic acid dehydratase from *Wolbachia* endobacteria. *Bioorg. Med. Chem. Lett.* **2013**, *23*, 5558−5562.
(24) Erskine, P. T.; Norton, E.; Cooper, J. B.; Lambert, R.; Coker, A.; Lewis, G.; Spencer, P.; Sarwar, M.; Wood, S. P.; Warren, M. J.; Shoolingin-Jordan, P. M. X-ray structure of 5-aminolevulinic acid dehydratase from *Escherichia coli* complexed with the inhibitor levulinic acid at 2.0 Å resolution. *Biochemistry* **1999**, *38*, 4266−4276.
(25) Jaffe, E. K.; Ali, S.; Mitchell, L. W.; Taylor, K. M.; Volin, M.; Markham, G. D. Characterization of the role of the stimulatory magnesium of *Escherichia coli* porphobilinogen synthase. *Biochemistry* **1995**, *34*, 244−251.
(26) Reitz, A. B.; Ramirez, U. D.; Stith, L.; Du, Y.; Smith, G. R.; Jaffe, E. K. *Pseudomonas aeruginosa* porphobilinogen synthase assembly state regulators: hit discovery and initial SAR studies. *ARKIVOC* **2010**, *2010*, 175−188.
(27) Bowman, D. D. Introduction to the alpha-proteobacteria: *Wolbachia* and *Bartonella*, *Rickettsia*, *Brucella*, *Ehrlichia*, and *Anaplasma*. *Top. Companion Anim. Med.* **2011**, *26*, 173−177.
(28) Henrichfreise, B.; Schiefer, A.; Schneider, T.; Nzukou, E.; Poellinger, C.; Hoffmann, T. J.; Johnston, K. L.; Moelleken, K.; Wiedemann, I.; Pfarr, K.; Hoerauf, A.; Sahl, H. G. Functional conservation of the lipid II biosynthesis pathway in the cell wall-less bacteria *Chlamydia* and *Wolbachia*: Why is lipid II needed? *Mol. Microbiol.* **2009**, *73*, 913−923.
(29) Jaffe, E. K.; Lawrence, S. H. The morpheein model of allostery: evaluating proteins as potential morpheeins. *Methods Mol. Biol.* **2012**, *796*, 217−231.
(30) Lawrence, S. H.; Jaffe, E. K. Expanding the concepts in protein structure−function relationships and enzyme kinetics: teaching using morpheeins. *Biochem. Mol. Biol. Educ.* **2008**, *36*, 274−283.
(31) Lawrence, S. H.; Ramirez, U. D.; Tang, L.; Fazliyez, F.; Kundrat, L.; Markham, G. D.; Jaffe, E. K. Shape shifting leads to small-molecule allosteric drug discovery. *Chem. Biol.* **2008**, *15*, 586−596.
(32) Lawrence, S. H.; Ramirez, U. D.; Selwood, T.; Stith, L.; Jaffe, E. K. Allosteric inhibition of human porphobilinogen synthase. *J. Biol. Chem.* **2009**, *284*, 35807−35817.
(33) Lawrence, S. H.; Selwood, T.; Jaffe, E. K. Diverse clinical compounds alter the quaternary structure and inhibit the activity of an essential enzyme. *ChemMedChem* **2011**, *6*, 1067−1073.
(34) Heinemann, I. U.; Schulz, C.; Schubert, W. D.; Heinz, D. W.; Wang, Y. G.; Kobayashi, Y.; Awa, Y.; Wachi, M.; Jahn, D.; Jahn, M. Structure of the heme biosynthetic *Pseudomonas aeruginosa* porphobilinogen synthase in complex with the antibiotic alaremycin. *Antimicrob. Agents Chemother.* **2010**, *54*, 267−272.
(35) Jaffe, E. K.; Shanmugam, D.; Gardberg, A.; Dieterich, S.; Sankaran, B.; Stewart, L. J.; Myler, P. J.; Roos, D. S. Crystal structure of *Toxoplasma gondii* porphobilinogen synthase: insights on octameric structure and porphobilinogen formation. *J. Biol. Chem.* **2011**, *286*, 15298−15307.
(36) McFadden, G. I. The apicoplast. *Protoplasma* **2011**, *248*, 641−650.
(37) Janouskovec, J.; Horak, A.; Obornik, M.; Lukes, J.; Keeling, P. J. A common red algal origin of the apicomplexan, dinoflagellate, and heterokont plastids. *Proc. Natl. Acad. Sci. U.S.A.* **2010**, *107*, 10949−10954.
(38) Obornik, M.; Green, B. R. Mosaic origin of the heme biosynthesis pathway in photosynthetic eukaryotes. *Mol. Biol. Evol.* **2005**, *22*, 2343−2353.
(39) Bechara, E. J.; Dutra, F.; Cardoso, V. E.; Sartori, A.; Olympio, K. P.; Penatti, C. A.; Adhikari, A.; Assuncao, N. A. The dual face of endogenous alpha-aminoketones: pro-oxidizing metabolic weapons. *Comp. Biochem. Physiol., Part C: Toxicol. Pharmacol.* **2007**, *146*, 88−110.
(40) Mitchell, L. W.; Jaffe, E. K. Porphobilinogen synthase from *Escherichia coli* is a Zn(II) metalloenzyme stimulated by Mg(II). *Arch. Biochem. Biophys.* **1993**, *300*, 169−177.
(41) Frankenberg, N.; Heinz, D. W.; Jahn, D. Production, purification, and characterization of a Mg^{2+}-responsive porphobilinogen synthase from *Pseudomonas aeruginosa*. *Biochemistry* **1999**, *38*, 13968−13975.